Crystallography and spin-crossover. A view of breathing materials

Philippe Guionneau

Crystallography and spin-crossover. A view of breathing materials

Philippe Guionneau[a,b]

The spin-crossover phenomenon (SCO) is a fascinating field that potentially concerns any material containing a (d^4–d^7) transition metal complex finding therefore an echo in as diverse research fields as chemistry, physics, biology and geology. Particularly, molecular and coordination-polymers SCO solids are thoroughly investigated since their bistability promises new routes towards a large panel of potential applications including smart pigments, optical switches or memory devices. Notwithstanding these motivating applicative targets, numerous fundamental aspects of SCO are still debated. Among them, the investigation of the structure–property relationships is unfailingly at the heart of the SCO research field. All the facets of the richness of the structural behaviors shown by SCO compounds are only revealed when exploring the whole sample scales – *from atomic to macroscopic* – all the external *stimuli* – *temperature, pressure, light and any combinations and derived perturbations* – and the various forms of the SCO compounds in the solid state – *crystalline powders, single-crystals, poorly crystalline or nano-sized particles*. Crystallography allows investigating all these aspects of SCO solids. In the past few years, crystallography has certainly been in a significant phase of development pushing the frontiers of investigations, in particular thanks to the progress in X-ray diffraction techniques. The encounter between SCO materials and crystallography is captivating, taking advantages from each other. In this paper, a personal account mainly based on our recent results provides perspectives and new approaches that should be developed in the investigation of SCO materials.

1. Introduction

The year 2012 has marked the centenary of the X-ray diffraction, XRD, discovery by von Laue *et al*. in 1912,[1] preceding the first crystal structure determination by Bragg in 1913;[2] in connection with these events, the General Assembly of the United Nations has elected the year 2014 as the International Year of Crystallography, marking one hundred years of XRD scrutiny of matter. Undoubtedly, thanks to the pioneering work of the last century, one of the keystones of modern science is the ability to determine the structures of any material (organic, inorganic, or biological) provided the crystalline powder or single-crystal forms are reachable. Nowadays, X-ray diffraction techniques are under constant improvement still pushing the frontiers of investigation. This is particularly true early in this century where, for example, recent X-ray diffraction technique developments applied to molecular materials allow investigation of local structures of samples showing poor crystallinity,[3] crystal structure modifications at the picosecond time scale,[4] the pressure–temperature phase diagrams[5,6] and very fine phenomena including incommensurate phases.[7] In the meantime, modern laboratory X-ray techniques and associated software make standard-quality crystal structure determination a routine step achievable by non-specialists who can refer to crystallographers when problems arise. One of the very positive consequences of this XRD development is that both the accuracy and the reachable number of structural information allow a deep knowledge of the physical phenomena affecting the crystalline materials and notably a study of the structure–property relationships. The determination of the latter is one of the crucial steps not only for the fundamental understanding of matter but also for the development of materials aimed at applications.

The investigation of molecular compounds strongly benefits from the impressive development of crystallography. The spin-crossover, SCO, phenomenon represents a fascinating example of how crystallography can play a crucial role not only for the fundamental understanding of the phenomenon but also as a guide along the route towards materials aimed at applications. In this paper, we will provide our tribute to the structural investigation of molecular iron(II) SCO materials from the atomic to the macroscopic scale, enlightening prospects. Beyond the study of SCO, this review aims at illustrating

[a]*University of Bordeaux, ICMCB, UPR 9048, F-33600 Pessac, France*
[b]*CNRS, Institute of Condensed Matter Chemistry of Bordeaux (ICMCB), UPR 9048, F-33600 Pessac, France. E-mail: guionneau@icmcb-bordeaux.cnrs.fr*

how crystallography can be efficiently used in many research fields of materials, especially if physical properties are connected with structural modifications, which is very often the case.

SCO corresponds to the switching of the electronic configuration of a transition metal compound between high spin (HS) and low spin (LS) states as a result of a perturbation. The latter can be of many kinds including modifications of temperature, pressure, light irradiation, magnetic and electric fields or pH. The SCO inevitably induces a switch of the magnetic, optical and structural properties of the material. The interplay between the properties of the material itself and the external conditions has been widely studied in the last 30 years, revealing a very complex phenomenon.[8–10] Whereas in solution the SCO takes place without cooperativity between metal centres resulting in a conversion that is always very gradual, in the solid state the conversion presents a large diversity of behaviours ranging from very abrupt with hysteresis to multi-step or incomplete reversible SCO for instance. It is therefore in the solid state that the SCO offers the best circumstances to investigate its fundamental aspects and to offer rational molecular engineering towards materials aimed at applications. Consequently, we focus here on the SCO occurring in the solid state, even though it is likely to be ultimately used and developed as well in solutions. The SCO is observable for the first-row transition metal elements with d^4–d^7 electronic configurations but is markedly more commonly studied in iron-containing compounds. In octahedral iron(II) complexes, the SCO is related to the electronic configuration of the ion switching from a paramagnetic HS ($S = 2$, $t_{2g}^4e_g^2$) to a diamagnetic LS ($S = 0$, $t_{2g}^6e_g^0$). This well-marked change of magnetic properties is one of the reasons why octahedral iron(II) complexes are the most studied so far. The SCO phenomenon takes place on the metal centres and then propagates all along the solid material across the different scales, including the structural ordering, up to the macroscopic scale. We will see here how crystallography allows description of the interplay between structural and physical properties, giving a picture of the SCO mechanism (section 2), notably thanks to the use of constrained environment XRD techniques to describe the phase diagrams (section 3) and how crystallography now challenges the exploration of poorly crystallized and nano-sized materials (section 4).

Philippe Guionneau

Philippe Guionneau received his PhD from the University of Bordeaux I (France) in 1996 under the supervision of Prof. D. Chasseau in the field of Condensed Matter, focusing on molecular conductors. He then joined Prof. J. A. K. Howard's group in Durham (UK) working on extreme-conditions crystallography. In 1998, he was appointed Assistant Prof. at the University of Bordeaux I in Prof. Olivier Kahn's group at the Institute of Condensed Matter Chemistry of Bordeaux (ICMCB). He is now a Professor at the University of Bordeaux, teaching physics, performing his research in the Molecular Science group and heading the X-ray diffraction centre of ICMCB. His present research mainly focuses on the structure–property relationships in functional molecular materials, notably molecular switches.

2. Multi-scale picture of the SCO breathing

SCO takes place on the metal centre driving structural consequences for the material at the various scales. Fig. 1 summarizes the different scales discussed below.

2.1 Metal site

The most obvious consequence of SCO on the metal site is the reversible shortening of the metal–ligand bond length from HS to LS (Fig. 1). The latter corresponds to a reversible

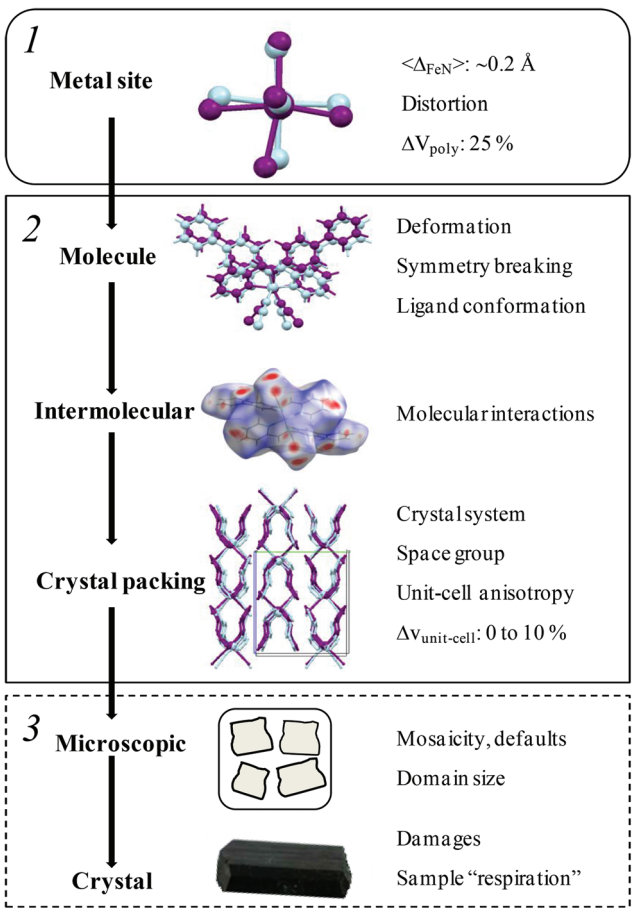

Fig. 1 Multi-scale view of the possible structural modifications connected with the SCO phenomenon going from the geometry of the coordination sphere – **1** example of the FeN_6 environment (HS in purple, LS in cyan) – to the molecule and the crystal packing – **2** example of $[Fe(PM\text{-}BiA)_2(NCS)_2$ – and up to the scale of the whole sample – **3** the crystal itself.

decrease of the Fe–N bond lengths by on average 0.2 Å, *i.e.* about 10%.[11–13] This large modification is directly observable from the atomic positions obtained from the crystal structure determination of the sample in the HS and LS states. The metal–ligand bond length is thus a sort of witness used to determine the spin state of a sample in a given environment. Furthermore, it is a nice tool to estimate all intermediate situations when the structure accommodates a mixture of HS and LS. Indeed, since the crystal structure determination gives an average view of the atomic positions on a given metal site when there is a random disorder on it, the resulting metal–ligand bond length reflects the proportion of the disorder. For example, in a HS FeN_6 environment, when there is a partial substitution by LS, the resulting Fe–N lengths lie in between the pure HS and the pure LS values in proportion to the LS substitution rate.

The metal–ligand bond length analysis was efficiently used in the variable temperature study of [Fe(picen)$(NCS)_2$] (where picen = *N*,*N*′-bis(2-pyridylmethyl)1,2-ethanediamine) to estimate the degree of SCO conversion as a function of the experimental protocol (Table 1).[14] SCO also affects the metal site by the modification of the ligand–metal–ligand angles resulting in a more regular polyhedron in LS (Fig. 1). Many tools for estimating the degree of distortion have been proposed. They mainly derive from systematic investigations of a family of iron(II) SCO complexes of general formula [Fe(PM-L)$_2(NCS)_2$] (where PM = *N*-2′-pyridylmethylene and L is an aromatic ligand).[12,15] Among them the angle distortion parameter, Σ, which represents the sum of the deviations from 90° of the 12 *cis* N–Fe–N angles in the FeN_6 coordination sphere, appears to be very different from one complex to another but is clearly spin-state dependent.[12,13,16] The length distortion parameter, ζ, defined as the sum of the deviations from the average value of all the Fe–N bond lengths, is also used to determine the polyhedron distortion.[17] Both parameters, Σ and ζ, are efficiently used to characterize the spin state of the metal. More interestingly, the distortion can also be investigated using the Θ parameter, defined as the sum of the deviations from 60° of the 24 possible octahedron twist angles.[18] This parameter, directly calculated from the crystal structures, is relevant since not only its value depends on the spin state but also it can be directly correlated to magnetic properties. Indeed, for example, it was shown from experimental structural data that the amplitude of the Θ modification at the SCO is almost linearly linked to T(LIESST). The latter is the temperature limit of photo-inscription determined from magnetic measurements following a precise protocol.[19,20] Recently, it was very exciting to see that pure theoretical considerations have validated the predominant role of the Θ distortion in the photo-induced SCO process.[21] As a general matter, the link between the metal coordination sphere distortion and the spin state of the metal was earlier underlined by theoretical considerations.[22] In parallel, systematic measurements of T(LIESST) in SCO materials have evidenced a connection between the photo-induced SCO temperature and the metal environment.[19] Such interplay is employed to design materials with higher temperature of photo-inscription. Note that the modification of the metal–ligand angles due to SCO is however not observed if the polyhedron appears already regular in the HS state, which happens in some geometries leading to a rigid metal-coordination sphere. This was already anticipated by theoretical considerations[21,22] and recently observed in the structural study of a SCO material based on infinite iron–triazole chains.[23] The latter show a regular FeN_6 octahedron in both HS and LS, with consequently no modification of the distortion parameters at the SCO in this case.

As a general feature, the modifications of the metal site geometry due to SCO affect the coordination sphere volume. As a consequence, since the SCO is perfectly reversible, the contraction–dilatation process of the metal site results in a *breathing* of the material. In the case of the FeN_6 polyhedron, the amplitude of the respiration, at the level of the metal site, is almost the same in all compounds and is, as calculated from structural data, $\Delta V_{poly} \sim 25\%$.[12,24,25]

Table 1 Calculation of the degree of SCO conversion in [Fe(picen)$(NCS)_2$] from the Fe–N bond lengths determined at 30 K depending on the cooling rate used from 120 to 30 K. Interpreted from ref. 14

T (K)	120	30	30	30	30
Cooling rate from 120 to 30 K (K h^{-1})	—	Instant	360	30	3
$\langle d_{Fe-N} \rangle$ (Å)	2.1750	2.1518	2.1038	2.0708	2.0316
Degree of HS→LS conversion (%)	0	12	36	52	72

2.2 Molecular scale

The *breathing* of the metal coordination sphere propagates to the whole molecule itself (Fig. 1). The structural impact of the SCO at this scale is very different from one sort of molecule to another and is hardly predictable. The molecular structural modifications notably depend on the flexibility of the ligands; some examples are shown in Fig. 2.

In the case of the family of [Fe(PM-L)$_2(NCS)_2$] complexes, the SCO from HS to LS strongly affects the aperture angle of the –(NCS) ligands.[12,15–20,26] From this point of view, in this family of materials, the SCO *breathing* at the molecular scale can be seen as like the flapping of a butterfly's wings (Fig. 2a). In contrast, in the case of the [Fe(abpt)$_2$] derivative complexes (abpt = 4-amino-3,5-bis(pyridin-2-yl)-1,2,4-triazole), the strong alteration of the metal coordination sphere is not propagated to the scale of the molecule and the geometry of the ligands appears to be similar in HS and LS (Fig. 2b).[27] In the case of the dinuclear [{Fe(3-bpp)$(NCS)_2$}$_2$(4,4′-bipyridine)] (bpp = 2,6-bis(pyrazol-3-yl) pyridine), the modifications affect mainly one side of the molecule inducing a dissymmetry (Fig. 2c).[28] An extreme case was encountered with the complex [Fe(L)$(CN)_2$]·H_2O (where L = [2,13-dimethyl-6,9-dioxa-3,12,18-triazabicyclo[12.3.1]-octa-deca-1(18),2,12,14,16-pentaene]) displaying an iron(II) that is heptacoordinated in HS.[29] The SCO strongly affects the molecule since there is an inversion of the O–CH_2–CH_2–O ethylene ring conformation together with a departure of one oxygen atom from the metal coordination sphere,

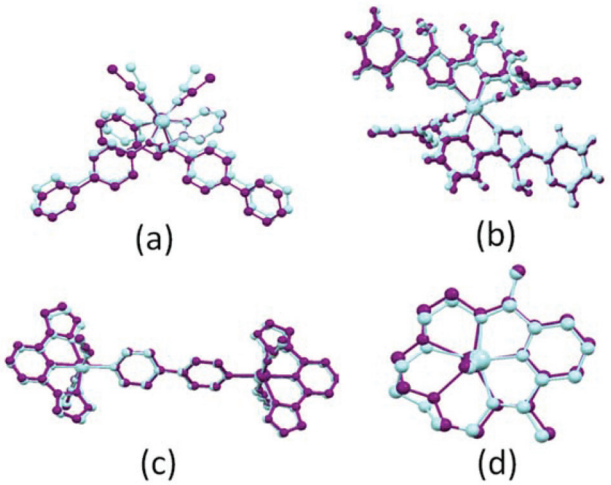

Fig. 2 Superposition of the molecular structures in HS (purple) and LS (cyan) extracted from the crystal structures of (a) $[Fe(PM\text{-}BiA)_2(NCS)_2]$,[26] (b) $[Fe\text{-}(abpt)_2]$,[27] (c) $[\{Fe(3\text{-}bpp)(NCS)_2\}_2(4,4'\text{-}bipyridine)]$[28] and (d) $[FeL(CN)_2]\cdot H_2O$.[29] See text for the full chemical names of the compounds.

resulting in a LS state together with a hexacoordinated iron (Fig. 2d). Consequently, in this case, the HS to LS SCO induces a metal–ligand bond breaking. The fascinating point is the perfect reversibility of this phenomenon even in the crystalline solid state. The above examples illustrate different ways in which the modifications at the metal scale can affect the whole molecule. The diversity of behaviours is even enhanced by the fact that the molecules are never strictly isolated in a crystal. The crystal cohesion comes from intermolecular interactions and consequently the molecular response to SCO is also influenced by intermolecular interactions.

2.3 Intermolecular interactions

The picture of the intermolecular interactions can be deeply modified by the SCO phenomenon and conversely the intermolecular interactions can influence the SCO features. It is well established now that the complexity of the SCO phenomenon in the solid state, in contrast to solutions, originates mostly from the interactions between molecules.[13] Depending on the nature of the complexes, hydrogen bonds or π–π stacking are often evidenced as playing a predominant role in the SCO characteristics.[13,15,27,30,31] For example, in the case of the $[Fe(PM\text{-}L)_2(NCS)_2]$ family, hydrogen bonds have been clearly shown to be responsible for the abruptness of the SCO.[15,26] An accurate description of intermolecular interactions is always necessary to understand the behaviour of a SCO material. Note that such an approach using crystallography data grows to its paroxysm when electronic density investigations are performed allowing a very fine description. This difficult and time consuming method was used in the study of some SCO iron(II) complexes and brought a new structure–property relationship for the investigated materials.[32] Nevertheless, the topology of the intermolecular interaction is diversely affected from one material to another. Recently, an exhaustive review published by Halcrow challenges to extract direct relations between the SCO features and the structural properties, notably intermolecular interactions.[13] If the role of the latter is clearly determined in the cooperativity of the SCO, no general correlation emerges, mainly due to the diversity of the structural situations.

Fig. 3 represents three examples of intermolecular contact topologies depicted through Hirshfeld surface analysis.[33] The latter allows an easy view of the possible intermolecular interactions in the crystal packing seen at the molecular level. In this figure, red spots designate intermolecular contact. Consequently a change of the number, position or intensity of the red spots corresponds to a modification of the intermolecular contact topology. The first example concerns the Mn(III) material [Mn(TRP)] (TRP = tris[1-(2-azolyl)-2-azabuten-4-yll-amine) undergoing an abrupt SCO that shows almost no incidence of the SCO on the intermolecular contacts, *i.e.* there is no significant modification of either the lengths or the number of intermolecular contacts as shown by Hirshfeld surfaces (Fig. 3a) and as confirmed by a thorough analysis of intermolecular distances and angles.[34] The second one deals with the complex $[Fe(PM\text{-}NeA)_2(NCS)_2]$ family (PM-NeA = *N*-(2-pyridyl methylene)-4-(naphthalene-1-ethynyl)aniline) and illustrates what is probably the most common situation, *i.e.* the

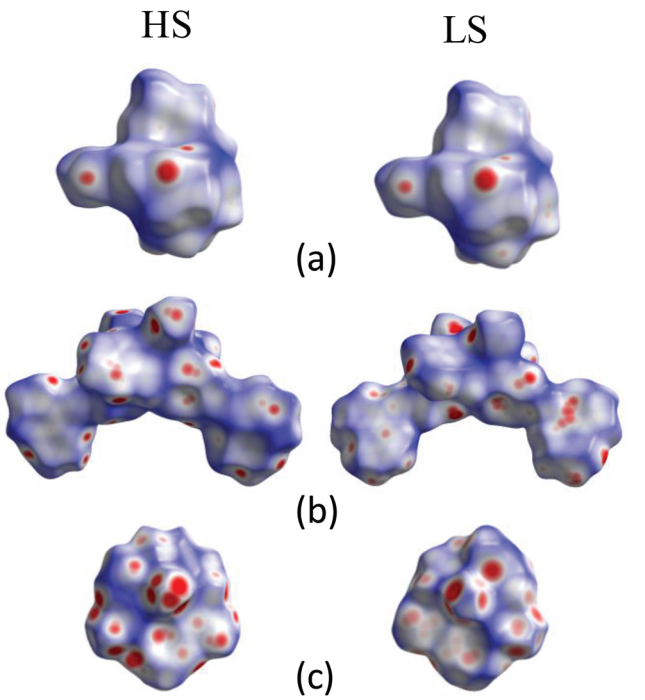

Fig. 3 Normalized intermolecular contacts mapped on the Hirshfeld surfaces in HS and LS of the SCO compounds (a) [Mn(TRP)],[34] (b) $[Fe(PM\text{-}NeA)_2(NCS)_2]$[35] and (c) $[FeL(CN)_2]\cdot H_2O$.[29] The colour scale describes the distances longer (blue), equal (white) or shorter (red) than the van der Waals radii. This figure has been obtained with the Crystal Explorer software[36] using the crystallographic data in cif file format extracted from the above references. See text for the full chemical names of the compounds.

number of intermolecular contacts is much higher in LS (Fig. 3b).[35] It also shows a strong spin-state dependence of the intermolecular contacts since they are largely modified in position and strength at the SCO. As a result, the cooperativity of the system is different in HS and LS. In this case, as very often, the cooperativity appears stronger in LS. In contrast, in the last example, based on the atypical $[FeL(CN)_2]\cdot H_2O$ complex already mentioned above (Fig. 2d),[29] SCO corresponds to a large modification of the envelope of the complex resulting in a less cooperative network in LS. The modifications of the intermolecular contacts are by definition hardly predictable and the diffraction method appears hence essential for establishing a correlation between the cooperativity of SCO and the intermolecular contact properties. However, a pertinent description of the latter is very often inextricable due to a too large number and a rich diversity of interactions in molecular materials. If one intermolecular contact is predominant and thus relatively easy to detect in the middle of all the contacts, direct structure–property relationships can be established. This is the case when the S···H–C intermolecular contact in the $[Fe(PM\text{-}L)_2(NCS)_2]$ family was directly connected to the SCO cooperativity.[12,26] When cooperativity cannot be so simply connected to a single structural parameter, the difficulty comes from the description of the whole intermolecular contacts, leading to long and fastidious distance and angle lists. As a recent example, an elegant solution has been proposed to simply and quantitatively describe this structural feature, the so-called crystal contact index.[31] The latter is based on the sum of all short and weighted contacts and has been used to correlate intermolecular interaction and cooperativity in a series of SCO materials.

Besides, the role of the intermolecular interactions and their modification to account for SCO features are also revealed when exploring the role of solvent molecules inserted within the crystal. In almost all cases, it is concluded that the solvents play a key role, through their interactions with complexes, in the propagation and occurrence of SCO in the material.[13,30] At this stage, it is worth noting another difficulty in the correlation between structural features and SCO. The latter needs a stimulus and/or a change of thermodynamic conditions to happen. It is thus sometimes difficult to disconnect the effects of the pure SCO from the effects of external perturbations on the structural features. An ideal situation comes up when it is possible to get an isostructural complex that does not undergo SCO and can thus be used as a kind of witness of the external perturbation effects. For example, the cobalt and zinc based complexes, $[Co(PM\text{-}L)_2(NCS)_2]$ and $[Zn(PM\text{-}L)_2(NCS)_2]$, were used to separate the pure thermal effects from those of SCO in the $[Fe(PM\text{-}L)_2(NCS)_2]$ family.[24,37,38] This approach should be generalized when possible. To conclude, the initial large modification of the metal coordination sphere, almost identical in all complexes, corresponds to structural variations different from one material to another. These variations affect the molecular geometry and its environment within the crystal packing, as revealed by the intermolecular contacts.

2.4 Crystal packing breathing

Another way to follow the structural modifications due to SCO is to look at the crystal packing globally through the unit cell parameter values (Fig. 1). This approach is common since unit-cells are directly accessible from diffraction experiments and it brings very interesting information. It allows for example to quantify the final amplitude of the SCO breathing on the material. The variation of the unit cell volume reflects the modification of the SCO material crystal packing (Fig. 4). Once the external perturbation effects are deduced, the amplitude of the unit cell volume variations due to SCO, denoted as $\Delta V_{\text{unit-cell}}$ (Fig. 1), varies usually from 1 to 5% in iron(II) complexes. In exceptional situations, this value can increase significantly, like in the polymeric SCO $[Fe(Htrz)_2(trz)](BF_4)$ (Htrz = 1*H*-1,2,4-triazole and trz = deprotonated triazolato ligand)

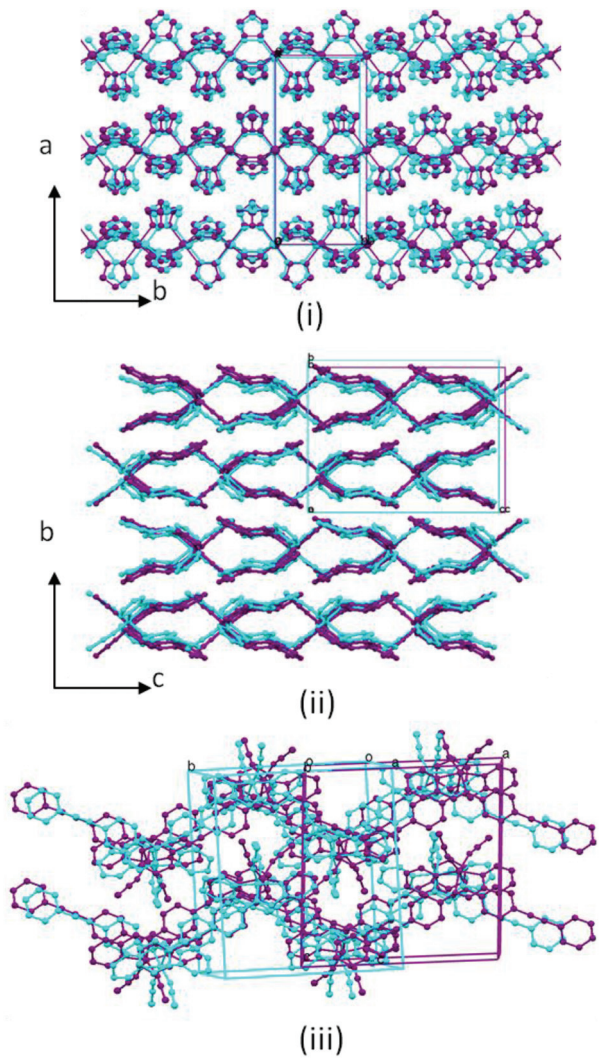

Fig. 4 Example of the superposition of the HS (purple) and LS (cyan) crystal packings of (i) the polymeric SCO material $[Fe(Htrz)_2(trz)](BF_4)$, (ii) the mononuclear $[Fe(PM\text{-}BiA)_2(NCS)_2]$ showing a gradual SCO and (iii) the mononuclear $[Fe(PM\text{-}PeA)_2(NCS)_2]$ showing a first order SCO transition (PM = *N*-2′-pyridylmethylene, BiA = 4-aminobiphenyl and PeA = 4-(phenylethynyl)aniline). Pictures are drawn from structural data in ref. 15, 23, 26.

compound where $\Delta V_{\text{unit-cell}}$ grows above 10%.[23] The latter value is impressive since it takes place in the solid state and corresponds to single-crystal respiration. Still, these changes are always smaller than the initial modification of the iron polyhedron (25%), the reason being the partial absorption of the contraction–dilatation by the crystal packing due to the accommodation of the molecule geometry, as discussed above.

As shown in Fig. 4 the respiration can also be strongly anisotropic with almost no modifications in one direction while most of the respiration is supported by another direction inside the crystal packing. In this regard, each compound is different and crystallographic investigations must be performed to give an accurate description of the sample SCO breathing. To this aim, the structural modifications associated with SCO are large enough to be followed by simple unit-cell temperature dependence. Nowadays, X-ray diffraction multi-temperature studies are routinely achievable and in some cases it is almost faster to obtain it than to correctly measure magnetic properties. Multi-temperature crystallography investigation using many experimental points all along the SCO path can now be performed systematically to get an accurate insight into the structural modifications associated with SCO in a quasi-continuous manner. In the study of $[Fe(L)](ClO_4)_2$ (where L = 1,4,7-tris(2-aminophenyl)-1,4,7-triazacyclononane), for instance, unit-cell measurements have been a straightforward tool to characterize gradual SCO.[25] The Bragg-peak temperature dependence is also now commonly used to determine the mechanism of the SCO itself, indicating the nature of the SCO phenomenon. Indeed, a gradual SCO corresponds to a continuous evolution of the Bragg peak positions while a first-order SCO corresponds to a splitting of the Bragg peaks with their relative intensity and not their changing positions with temperature.[39] The interpretation of X-ray diffraction patterns from multi-temperature investigations is however not always straightforward, notably in the case of twinings,[40] superstructures[41] or incommensurate transformations[42] that are associated with the SCO. There is no doubt however that these kinds of investigations will tend to grow in the next few years, probably revealing new facets of the structure–property relationship in SCO materials.

2.5 The microscopic and macroscopic scales

The magnitude of the crystal packing *respiration* due to SCO is not necessarily, and in fact is probably never, fully propagated at the macroscopic scale. That would be the case only for an ideal single-crystal composed of a unique domain without any defects of any kind. Probably this does not exist. Between the crystal packing and the macroscopic scales, many phenomena can occur at the microscopic level. Apart from breaking or damaging the sample, the presence of microscopic defects may strongly influence the way the SCO propagates at the macroscopic level. Even though these considerations are quite new in the SCO field, thorough studies by means of optical[43] and/or atomic force[44] microscopies have been recently performed on single crystals to emphasise the complexity of the propagation of the SCO at the macroscopic level. Conversely,

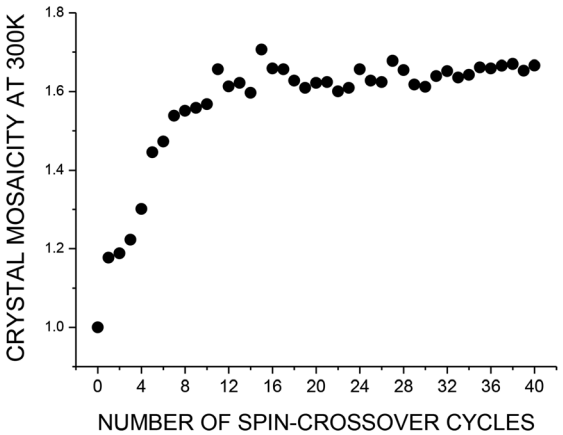

Fig. 5 Modification of the single-crystal mosaicity as a function of the number of thermal SCO undergone by the sample. The increase of mosaicity determined by X-ray diffraction at 300 K corresponds to structural fatigability of the sample. The figure is modified from ref. 38.

very few crystallographic studies have been attempted on this topic and the role of structural defects in the SCO is yet to be explored. This is an important topic with fundamental interest obviously, but also it touches some of the crucial questions that concern the use of SCO materials for applications and mainly the question of the fatigability of the SCO phenomenon. Recently, as a preliminary investigation, we have observed that the mosaicity of a single crystal was strongly altered after only a few SCO cycles showing thus fatigability although the studied complex showed a very gradual SCO (Fig. 5).[38] Tools exist in crystallography to deeply investigate the microscopic scale through the study of structural defects. For example, powder diffraction techniques appear more pertinent to quantify structural defects and micro-constraints in a sample and therefore their modifications due to SCO. This approach is one of the further contributions that crystallography must bring to the SCO field.

3. Multi-environment (*T*, *P*, *hν*) and SCO

The richness of the SCO phenomenon also comes from the many different stimuli used since SCO can be triggered by temperature, pressure or light effects. Consequently, investigation of the physical and structural properties in various environments allowing different kinds of perturbations is required.

3.1 Photo-crystallography and SCO

The photo-induced SCO was observed almost three decades ago and named as the LIESST effect.[45] Since then, numerous experimental and theoretical studies have been performed giving rise nowadays to a proper field of investigation.[4,8,9,19,20,32,42] Following structural investigations concerning unit-cell parameter dependence under light irradiation,[46] the first crystal structure of a SCO material in a light-induced HS state was determined about a decade ago.[47]

One of the consequences of this earlier work was to experimentally establish the link between the distortion of the metal-coordination sphere and the photo-induced SCO properties.[18] A high distortion corresponds to a high temperature of photo-conversion. Such an assumption was also largely explored by photo-magnetism measurements,[19,20] used for the design of new materials[13] and recently confirmed by theoretical approaches.[21,48] Photo-crystallography by means of X-ray diffraction is presently a very dynamic area and is intensively applied to the study of SCO materials. This approach has been demonstrated to be powerful provided some experimental cautions.[49] Also, it is used to deeply investigate the SCO mechanism itself.[17,32,50] As discussed above, one of the main difficulties of the structure–property correlations using structural data from the thermal SCO is indeed the differentiation between pure thermal and SCO features. Investigating the photo-induced SCO allows, thus, to suppress this difficulty since the HS to LS relaxation process, corresponding to the recovery of the thermal equilibrium state once the light is switched off, is performed at fixed temperature. The characteristics of the light used in the experiment must be well controlled and chosen since it strongly influences the result. Significant breakthroughs on the SCO mechanism using photo-crystallography, including the observation of phase separation processes, have been recently reviewed.[50] In parallel, photo-crystallography of SCO material has allowed pushing the frontiers of crystallography itself. Indeed, ultrafast time-resolved crystallography has been notably developed for the study of the SCO photoswitching dynamics through the work of Collet *et al.*[4,50] This fascinating field allows to obtain structural information at the picosecond time scale and has allowed a first view of the pathway of the structural reorganisation corresponding to the HS to LS relaxation.[51] The description of such a pathway appears crucial to control the macroscopic photoswitching in SCO materials not only because of the fundamental interest but also because, as we can recall, the photo-induced SCO is expected to be the most probable area of application of SCO materials.[10,52] Ultrafast time-resolved crystallography has also underlined the complexity of the structural dynamic processes associated with the photo-induced SCO, featuring exciting challenges using the next generation of X-ray sources notably to get to the femtosecond time scale.[50]

3.2 Piezo-crystallography and SCO

The role of pressure in SCO has been widely explored by theoretical approaches.[53] The application of pressure is likely to favour the LS state, the temperature of SCO increasing linearly with pressure while the hysteresis width decreases. However many experimental results, based on spectroscopies or magnetic measurements, have shown counter-examples as well as unexpected or contradictory behaviours.[50] In all cases, the potential role of pressure-induced structural transitions was emphasized, requiring crystallography data under pressure.

As a matter of fact, the access to relatively simple X-ray diffraction high pressure investigations has been only recently made available thanks to the adaptation of the use of diamond anvil cells (DAC) to two-dimensional detector experiments. Many recent reviews underline the actual dynamics of this field, showing the progress of crystallography under pressure.[54] Concerning SCO, in spite of some pioneering studies performed two decades ago,[55] it is only in the last few years that substantial high-pressure structural results were obtained, though they are still rare enough.[50] High pressure diffraction experiments were performed on six mononuclear or dinuclear SCO materials so far, giving accurate structural data in the range of 0–30 kbar. In many cases, unexpected behaviours were enhanced by crystallographic investigations leading to the conclusion that the pressure effects on SCO materials are almost unpredictable. For example in the case of the mononuclear SCO Fe(II) complexes of the formula $[Fe(PM\text{-}BiA)_2(NCS)_2]$, known to present an unexpected magnetic behaviour under pressure,[56] we found that the application of pressure favours the transformation to a polymorph showing very different SCO features. This partially explains the non-conventional magnetic behaviour previously observed.[57–59] An example of the discrepancy between thermal and pressure SCO behaviours is given by the dinuclear complex $[\{Fe(bpp)(NCS)_2\}_2]$4,4′-bipyridine]·2MeOH that shows a partial SCO at ambient pressure while the application of pressure allows a complete SCO.[28] Following the high pressure single-crystal structural investigation on this material, this discrepancy has been attributed to a purely structural phase transition occurring at low temperature but that is strongly disfavoured by high pressure.[60] One of the most spectacular behaviours revealed by a high pressure structural investigation of a SCO material likely concerns the $[Fe(dpp)_2(NCS)_2]$·py complex (dpp = dipyrido[3,2-*a*:2′3′-*c*]phenazine and py = pyridine) that shows an antagonism between a negative linear compression (NLC) and SCO. The NLC originates from a scissor-like motion of the molecular complex resulting in a suppression of the SCO phenomenon under pressure.[61] Note that in some cases, the application of pressure on the SCO materials fulfilled the expectation, even when structural transitions are involved.[41] As a result, high-pressure structural investigation represents nowadays a necessary step to understand, and subsequently to use, the interplay between SCO and pressure.

3.3 SCO phase diagrams

The true challenge is to draw the temperature–pressure–light (P, T, $h\nu$) phase diagrams of SCO materials (Fig. 6). The archetype of this phase diagram was obtained with the $[Fe(phen)_2(NCS)_2]$ complex (phen = 1,10-phenanthroline) thanks to X-ray diffraction investigations at low temperature, high pressure and under irradiation.[47,49,55] This compound shows the expected SCO behaviours, and no drastic or unexpected structural transformations associated with SCO or with the modification of the external conditions are noticed (Fig. 6a). For instance, the symmetry of the crystal packing is unchanged all along the SCO pathway. Since the early stage of the SCO

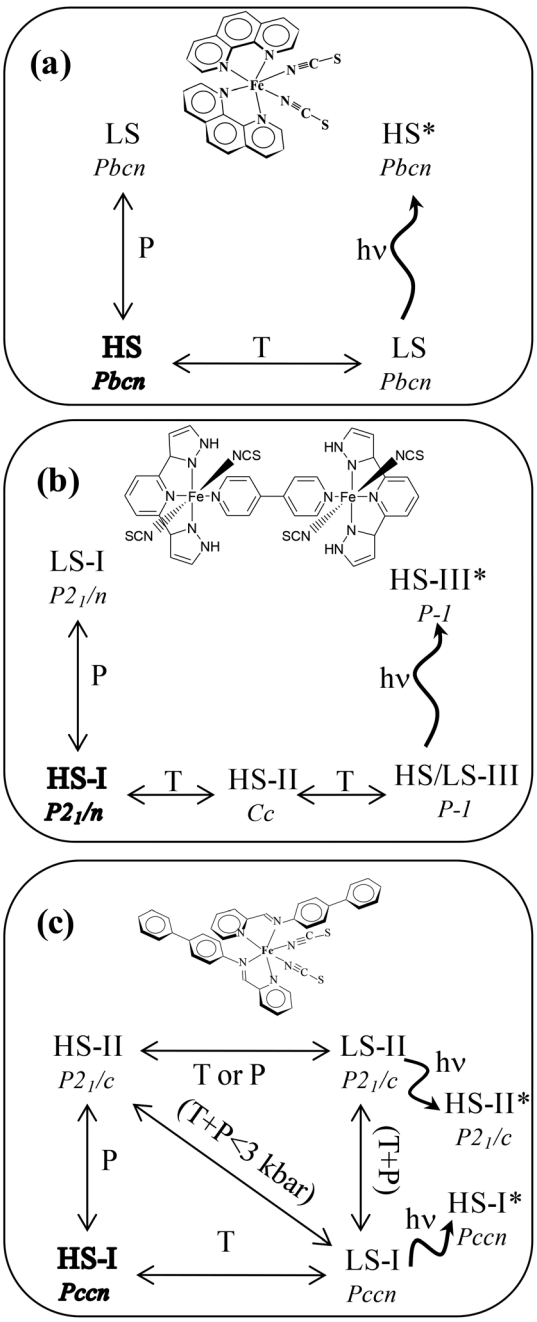

Fig. 6 Schematic views of the (*P*, *T*, *hν*) phase diagrams of some SCO materials: (a) $[Fe(phen)_2(NCS)_2]$ from ref. 47, 55, (b) $[\{Fe(bpp)(NCS)_2\}_2$4,4′-bipyridine]·2MeOH from ref. 28, 60 and (c) $[Fe(PM\text{-}BiA)_2(NCS)_2]$ from ref. 17, 26, 57–59. Molecular schemes are inserted. Code: HS for high spin, LS for low spin, P for pressure, T for temperature, *hν* for light irradiation and "*" to signal a light-induced spin state. Labels I, II and III indicate different structural phases; space groups are provided. See text for the full chemical names of the compounds.

phenomenon investigation, this compound is considered as a model for the SCO materials. In fact, it is probably one of the rare compounds to show a so simple (*P*, *T*, *hν*) phase diagram, at least from the complexes so far investigated.[50] For example, the phase diagram of the dinuclear complex $[\{Fe(bpp)(NCS)_2\}_2$4,4′-bipy]·2MeOH, already mentioned above, presents an interplay between spin state and structural phases (Fig. 6b). Depending on the external conditions, the sample can be obtained in the full HS state in not less than three different structural phases showing diverse space-groups and unit-cells. The full LS state can only be reached if pressure is applied and a crystalline phase with a mixture of ordered HS/LS complexes is obtained at ambient pressure. The role of the planarity of the bipyridine ligand was shown to be one of the key features to explain such a multifaceted phase diagram.[28,60] Since the access to low-temperature accurate structural data at high pressure is still problematic[6] in practice on SCO molecular materials the combination of crystallography with other approaches is required to establish the structural phase diagram of a compound. For example, in some cases, Raman spectroscopy under pressure was efficiently used to probe the spin state in order to determine the pressure domain to be explored in the X-ray investigation.[41,60–62] Elsewhere, a theoretical approach starting from structural data and based on DFT and molecular dynamic calculations has been recently used to complete the peculiar (*P*, *T*, *hν*) phase diagram of $[Fe(PM\text{-}BiA)_2(NCS)_2]$. Indeed, powder neutron diffraction under pressure previously revealed the pressure-induced transformation from an orthorhombic to a monoclinic polymorph.[57] Both polymorphs can also be synthesized independently and were already described including the structure–property correlation for the thermal SCO.[26] Taking the experimental isobaric and isothermal structural parameters dependence, theoretical calculations using DFT and molecular dynamics approaches allowed to describe the full (*P*, *T*) zones that the experiment hardly reaches.[59] The completed phase diagram revealed the possible transformation from one polymorph to another together with a change of the spin state, from LS-I to HS-II (Fig. 6c), at low temperature and moderate pressure. This intricate interplay between pressure, polymorphism and spin state has therefore been first seen by crystallography under pressure and then extrapolated by theoretical models. Some features of this calculated phase-diagram have been recently confirmed by neutron diffraction combining low temperature and high pressure.[58] For almost all SCO materials fully investigated in the (*P*, *T*) phase diagram so far, the resulting pattern appears complex. It involves antagonism or synergy between the structural modifications induced by the change of thermodynamic conditions and those induced by the SCO phenomenon itself. Once more, these results emphasize the important role of crystallography in the investigation of SCO.

4. SCO devices and crystallography

Fundamental investigation of SCO materials as described above, especially when talking about crystallography, is mostly performed on single crystals since it allows getting accurate, unambiguous and reliable structural data. However when looking for SCO devices, it is highly probable that the material would be used also in other forms such as poorly-crystalline powders or nano-sized samples. The limits of classical

crystallography appear then to be reached; nevertheless crystallography can help a lot to investigate and subsequently control the developments of SCO materials for applications.

4.1 From molecules to polymers

Coordination polymers have always been announced as the most promising SCO materials for applications.[10,52,63,64] Coordination polymers are metal–ligand compounds that extend infinitely at least in one dimension *via* covalent metal–ligand bonding.[65] In the case of SCO materials, a family of triazole based one-dimensional coordination polymers has been identified at least for two decades as fulfilling several of the requirements for applications, including room temperature SCO with large hysteresis.[66] This large family of the general formula $[Fe(Rtrz)_3][A]_2{\cdot}xH_2O$ (R = NH_2 or H; trz = 1,2,4-triazole) has been intensively studied in the past few years as stated in recent reviews.[10,63,64,67] Until very recently, the weak point of this family was that almost no structural information was known. Indeed, these coordination polymers are only obtainable in the form of poorly crystalline powders or small particules. During the last few decades, very partial structural information coming from X-ray absorption measurements were available and only confirmed the presence of "infinite" $Fe(Rtrz)_3$ chains in these compounds.[68] Very recently, following numerous trials that provided preliminary results[69] and due to significant progress in the chemical synthesis of these compounds but overall thanks to progress in X-ray diffraction techniques and data analysis we were able to provide the first reliable crystal structures of $[Fe(Rtrz)_3][A]_2{\cdot}xH_2O$ materials. These results were obtained either by applying single-crystal X-ray diffraction to very small samples with two dimensions inferior to 1 μm or by pushing powder X-ray diffraction to its limits in terms of data analysis.[23,70] Therefore the first description of the crystal packing of these SCO coordination polymers was proposed (Fig. 7). It revealed some unexpected properties such as the strong involvement of anions in the crystal cohesion, the very large unit-cell volume change at the SCO (>10%) or the reversible motion of the chains associated with the SCO. It also confirmed some expected features such as the strong anisotropy of these materials and the rigidity of the metal coordination sphere, probably at the origin of the absence of LIESST effects in this family of materials. Crystallography is thus able nowadays to reveal the crystal structure of samples that were considered until recently as poorly crystalline. As a general matter of fact, this statement calls for a re-investigation of many unsolved problems in the field of molecular materials. As a consequence on SCO materials, the route to systematic and accurate structural studies of SCO coordination polymers is now open with the aim of understanding the structure–property relationship in these promising materials.

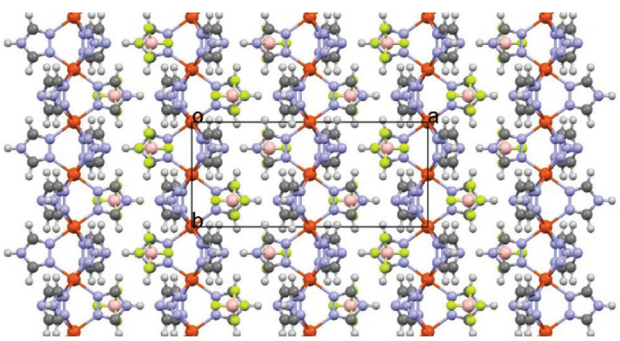

Fig. 7 View along *c* of the X-ray diffraction crystal structure of the SCO coordination polymer $[Fe(Htrz)_2(trz)](BF_4)$ built from "infinite" $Fe(Htrz)_2(trz)$ based chains along *b* linked by close contacts along *a* notably mediated by the BF_4 anions.[23]

4.2 Poorly crystallized and nano-sized materials

Poorly crystallized material can release some information even when studied by X-ray diffraction. It is also the case for nano-sized materials. The former are frequently encountered in the synthesis of new SCO compounds and the latter are obviously in fashion in the SCO field when talking about applicative materials.[10,63,71] Classical X-ray powder diffraction can anyhow give microscopic, interesting structural data on both kinds of "non-diffracting" systems. Among them the size of the coherent domains is reachable, providing careful experimental and data analysis. For example, in the study of the SCO material $[Fe(NH_2\text{-}trz)_3]Br_2{\cdot}3H_2O$ the coherent domain sizes of different batches, including poorly crystallized and nano-sized particle powders, were determined and compared to the particle sizes obtained by TEM.[72] This study revealed that, for this compound at least, the number of coherent domains per particle and not the coherent domain size appears to be the key factor for the existence of the SCO thermal hysteresis. As a general perspective, the investigation of microscopic structural data in relation to SCO features must be more thoroughly investigated in order to guide the design of SCO materials. To this aim, one of the new tools that have started to come out is the pair-distribution-function (PDF) approach.[3] This method based on high quality powder X-ray diffraction measurements allows getting local structural information for any kind of material including nanoparticles. It has been recently used in the study of a SCO material to compare the crystal structures of bulk (micro-sized particles) and nanoparticles.[23] This approach is probably one of the strongest answers to crystallography-derived techniques for the study of nano-objects and can be incidentally a method to investigate the role of defects in SCO materials by access to local structures (see section 2.5).

5. Conclusions

The aim of this Perspective was not only to show the contribution of crystallography to the knowledge of the SCO phenomenon but overall to underline that crystallography allows exploring new aspects of SCO materials thanks to the opening of new frontiers of investigation. After a few decades of study, the SCO research field attracts presently deep interest all over the world as shown by the large number of related recent reviews, special-issues and books.[9,10,63,64,67,73] From the structural point of view, following an initial period dedicated

to the determination of the crystal structures, yet a crucial step since, as a general matter, crystal structures remain almost unpredictable,[74] the exploration of structural properties of SCO materials will now be mainly concentrated on other physical scales – *including microstructures* – on a new time-scale for probing the structural modifications – *far shorter than the nanoscale* – on other thermodynamic conditions – *particularly high pressure* – and on other forms of SCO solids – *like poorly crystalline powders or nano-sized particles*. Recent developments of X-ray or neutron diffraction techniques, including ultrafast time-resolved XRD to powder diffraction methods or combined pressure–(low) temperature environments, permit exploring these facets of the structure–property relationship. These explorations should contribute to a deeper understanding of the SCO phenomenon and therefore can ultimately help in designing SCO materials adequate for applicative purposes. In this paper, through the structural description, only an oriented view of the SCO phenomenon is given but the manner in which the structural-properties are investigated may probably be extended to many other research fields related to organic or inorganic materials showing modifications under a *stimulus*, taking advantage of the present dynamism of crystallography.

Acknowledgements

All co-authors cited below in the reference list as well as all colleagues from the Science Molecular Group and the X-Ray Centre of ICMCB (France) are warmly acknowledged. Particular thanks are due to J.F. Létard for a fruitful collaboration on SCO materials and to the PhD students who worked on SCO with me, M. Marchivie, J. Sanchez-Costa, F. Le Gac, S. Lakhloufi and A. Grosjean. Many thanks are due to Dr Samir Matar for scientific discussions as well as for checking the English language in the manuscript. This work was supported by the University of Bordeaux, the CNRS and the Région Aquitaine.

Notes and references

1 W. Friedrich, P. Knipping and M. Laue, *Ann. Phys.*, 1913, **41**, 971.
2 W. L. Bragg, *Proc. R. Soc. London, Ser. A*, 1913, **89**, 248.
3 S. J. J. Billinge and M. G. Kanatzidis, *Chem. Commun.*, 2004, 749.
4 H. Cailleau, M. Lorenc, L. Guérin, M. Servol, E. Collet and M. Buron-Le Cointe, *Acta Crystallogr., Sect. A: Fundam. Crystallogr.*, 2010, **66**, 189.
5 A. Dawson, D. R. Allan, S. Parsons and M. Rulf, *J. Appl. Crystallogr.*, 2004, **37**, 410.
6 P. Guionneau, D. Lepevelen, M. Marchivie, S. Pechev, J. Gaultier, Y. Barrans and D. Chasseau, *J. Phys.: Condens. Matter*, 2004, **16**, 1129.
7 B. Toudic, P. Garcia, C. Odin, P. Rabiller, C. Ecolivet, E. Collet, P. Bourges, G. J. McIntyre, M. D. Hollingsworth and T. Breczewski, *Science*, 2008, **319**, 69.
8 *Spin-Crossover in Transition Metal Compounds I-III*, ed. P. Gütlich and H. A. Goodwin, *Top. Curr. Chem.*, Springer Verlag, Berlin/Heidelberg, Germany, 2004, pp. 233–235.
9 *Spin-Crossover Materials: Properties and Applications*, ed. M. A. Halcrow, John Wiley & Sons, 2013.
10 A. Bousseksou, G. Molnár, L. Salmon and W. Nicolazzi, *Chem. Soc. Rev.*, 2011, **40**, 3313; P. Gütlich, A. B. Gaspar and Y. Garcia, *Beilstein J. Org. Chem.*, 2013, **9**, 342.
11 E. König, *Prog. Inorg. Chem.*, 1987, **35**, 527; E. König, G. Ritter and S. H. Kulshreshtha, *Chem. Rev.*, 1985, **85**, 219; P. Gütlich, *Struct. Bonding*, 1981, **44**, 83.
12 P. Guionneau, M. Marchivie, G. Bravic, J.-F. Létard and D. Chasseau, *Top. Curr. Chem.*, 2004, **234**, 97.
13 M. A. Halcrow, *Chem. Soc. Rev.*, 2011, **40**, 4119.
14 J. F. Létard, S. Asthana, H. J. Shepherd, P. Guionneau, A. E. Goeta, N. Suemura, R. Ishikawa and S. Kaizaki, *Chem.–Eur. J.*, 2012, **18**, 5924.
15 P. Guionneau, J. F. Létard, D. S. Yuffit, D. Chasseau, J. A. K. Howard, A. E. Goeta and O. Kahn, *J. Mater. Chem.*, 1999, **4**, 985; J. F. Létard, P. Guionneau, L. Rabardel, J. A. K. Howard, A. E. Goeta, D. Chasseau and O. Kahn, *Inorg. Chem.*, 1998, **37**, 4432; J. F. Letard, S. Montant, P. Guionneau, P. Martin, A. Le Calvez, E. Freysz, D. Chasseau, R. Lapouyade and O. Kahn, *Chem. Commun.*, 1997, 745; J. F. Létard, P. Guionneau, E. Codjovi, L. Olivier, G. Bravic, D. Chasseau and O. Kahn, *J. Am. Chem. Soc.*, 1997, **199**, 10861.
16 P. Guionneau, C. Brigouleix, Y. Barrans, A. E. Goeta, J.-F. Létard, J. A. K. Howard, J. Gaultier and D. Chasseau, *C. R. Acad. Sci. Paris, Chem.*, 2001, **4**, 161; J. K. McCusker, A. L. Rheingold and D. N. Hendrickson, *Inorg. Chem.*, 1996, **35**, 2100.
17 M. Buron-Le-Cointe, J. Hébert, C. Baldé, N. Moisan, L. Toupet, P. Guionneau, J. F. Létard, H. Cailleau and E. Collet, *Phys. Rev. B: Condens. Matter*, 2012, **85**, 064114.
18 M. Marchivie, P. Guionneau, J. F. Létard and D. Chasseau, *Acta Crystallogr., Sect. B: Struct. Sci.*, 2005, **61**, 25.
19 J.-F. Létard, P. Guionneau, O. Nguyen, J. S. Costa, S. Marcen, G. Chastanet, M. Marchivie and L. Capes, *Chem.–Eur. J.*, 2005, **11**, 4582; J.-F. Létard, *J. Mater. Chem.*, 2006, **16**, 2550.
20 J. F. Létard, G. Chastanet, P. Guionneau and C. Desplanches, Optimizing the Stability of Trapped Metastable Spin States, in *Spin-Crossover Materials: Properties and Applications*, ed. M. A. Halcrow, John Wiley & Sons Ltd, Oxford, UK, 2013, ch. 19, p. 475.
21 C. Boilleau, N. Suaud and N. Guihery, *J. Chem. Phys.*, 2012, **137**, 224304.
22 S. Alvarez, *J. Am. Chem. Soc.*, 2003, **125**, 6795.
23 A. Grosjean, P. Négrier, P. Bordet, C. Etrillard, D. Mondieig, S. Pechev, E. Lebraud, J. F. Létard and P. Guionneau, *Eur. J. Inorg. Chem.*, 2013, 796.

24 P. Guionneau, M. Marchivie, G. Bravic, J. F. Létard and D. Chasseau, *J. Mater. Chem.*, 2002, **12**, 2546.

25 H. J. Shepherd, P. Rosa, I. A. Fallis, P. Guionneau, J. A. K. Howard and A. E. Goeta, *J. Phys. Chem. Solids*, 2012, **73**, 193.

26 M. Marchivie, P. Guionneau, J. F. Létard and D. Chasseau, *Acta Crystallogr.*, 2003, **59**, 479; J. F. Létard, G. Chastanet, O. Nguyen, S. Marcen, M. Marchivie, P. Guionneau, D. Chasseau and P. Gütlich, *Monatsh. Chem.*, 2003, **134**, 165.

27 G. Dupouy, M. Marchivie, S. Triki, J. Sala-Pala, J. Y. Salaun, C. J. Gomez-Garcia and P. Guionneau, *Inorg. Chem.*, 2008, **47**, 8921.

28 A. Kaiba, H. J. Shepherd, D. Fedaoui, P. Rosa, A. E. Goeta, N. Rebbani, J. F. Létard and P. Guionneau, *Dalton Trans.*, 2010, **39**, 2910.

29 P. Guionneau, F. Le Gac, A. Kaiba, J. Sanchez-Costa, D. Chasseau and J. F. Létard, *Chem. Commun.*, 2007, 3723.

30 J. A. Real, A. B. Gaspar, V. Niel and M. C. Munoz, *Coord. Chem. Rev.*, 2003, **236**, 121; G. Lemercier, N. Brefuel, S. Shova, J. A. Wolny, F. Dahan, M. Verelst, H. Paulsen, A. X. Trautwein and J.-P. Tuchagues, *Chem.–Eur. J.*, 2006, **12**, 7421; M. Hostettler, K. W. Törnroos, D. Chernyshov, B. Vangdal and H.-B. Bürgi, *Angew. Chem., Int. Ed.*, 2004, **33**, 4589; C.-F. Sheu, S. Pillet, Y.-C. Lin, S.-M. Chen, I.-J. Hsu, C. Lecomte and Y. Wang, *Inorg. Chem.*, 2008, **47**, 10866; G. S. Matouzenko, E. Jeanneau, A. Y. Verat and Y. de Gaetano, *Eur. J. Inorg. Chem.*, 2012, **6**, 969; G. S. Matouzenko, E. Jeanneau, A. Y. Verat and A. Bousseksou, *Dalton Trans.*, 2011, **40**, 9608; H. V. Phan, P. Chakraborty, M. M. Chen, Y. M. Calm, K. Kovnir, L. K. Keniley, J. M. Hoyt, E. S. Knowles, C. Besnard, M. W. Meisel, A. Hauser, C. Achim and M. Shatruk, *Chem.–Eur. J.*, 2012, **18**, 15805; T. M. Ross, B. Moubaraki, D. R. Turner, G. J. Halder, G. Chastanet, S. M. Neville, J. D. Cashion, J. F. Létard, S. R. Batten and K. S. Murray, *Eur. J. Inorg. Chem.*, 2011, 1395.

31 T. A. Pfaffeneder, S. Thallmair, W. Bauer and B. Weber, *New J. Chem.*, 2011, **35**, 691.

32 S. Pillet, V. Legrand, H. P. Weber, M. Souhassou, J. F. Létard, P. Guionneau and C. Lecomte, *Z. Kristallogr.*, 2008, **223**, 235; V. Legrand, S. Pillet, M. Souhassou, N. Lugan and C. Lecomte, *J. Am. Chem. Soc.*, 2006, **128**, 13921.

33 M. A. Spackman and D. Jayatilaka, *CrystEngComm*, 2009, **11**, 19.

34 P. Guionneau, M. Marchivie, Y. Garcia, J. A. K. Howard and D. Chasseau, *Phys. Rev. B: Condens. Matter*, 2005, **72**, 214408.

35 J. F. Létard, M. Kollmansberger, C. Carbonera, M. Marchivie and P. Guionneau, *C. R. Chim.*, 2008, **11**, 1155.

36 S. K. Wolff, D. J. Grimwood, J. J. McKinnon, M. J. Turner, D. Jayatikala and M. A. Spackman, *Crystal Explorer*, University of Western Australia, Crowley, 2007.

37 F. Le Gac, P. Guionneau, J. F. Létard and P. Rosa, *Inorg. Chim. Acta*, 2008, **361**, 3519.

38 P. Guionneau, S. Lakhloufi, M. H. Lemée-Cailleau, G. Chastanet, P. Rosa, C. Mauriac and J. F. Létard, *Chem. Phys. Lett.*, 2012, **542**, 52.

39 A. Goujon, B. Gillon, A. Debede, A. Cousson, A. Gukasov, J. Jeftic, G. J. McIntyre and F. Varret, *Phys. Rev. B: Condens. Matter*, 2006, **73**, 104413; V. Legrand, S. Pillet, C. Carbonera, M. Souhassou, J. F. Létard, P. Guionneau and C. Lecomte, *Eur. J. Inorg. Chem.*, 2007, 5693; P. Guionneau, F. Le Gac, S. Lakhloufi, A. Kaiba, D. Chasseau, J. F. Létard, P. Négrier, D. Mondieig, J. A. K. Howard and J. M. Léger, *J. Phys.: Condens. Matter*, 2007, **19**, 32611; K. Ichiyanagi, J. Hebert, L. Toupet, H. Cailleau, P. Guionneau, J. F. Létard and E. Collet, *Phys. Rev B: Condens. Matter*, 2006, **73**, 060408.

40 J. Kusz, M. Zubko, R. B. Neder and P. Gütlich, *Acta Crystallogr., Sect. B: Struct. Sci.*, 2012, **68**, 40.

41 S. Pillet, E. Bendeif, S. Bonnet, H. J. Shepherd and P. Guionneau, *Phys. Rev. B: Condens. Matter*, 2012, **86**, 064106.

42 E. Collet, H. Watanabe, N. Bruefel, L. Palatinus, L. Roudaut, L. Toupet, K. Tanaka, J. P. J. Tuchagues, P. Fertey, S. Ravy, B. Toudic and H. Cailleau, *Phys. Rev. Lett.*, 2012, **109**, 257206.

43 A. Slimani, F. Varret, K. Boukheddaden, C. Chong, H. Mishra, J. Haasnoot and S. Pillet, *Phys. Rev. B: Condens. Matter*, 2011, **84**, 094442; A. Goujon, F. Varret, K. Boukheddaden, C. Chong, J. Jeftic, Y. Garcia, A. D. Naik, J. C. Ameline and E. Collet, *Inorg. Chim. Acta*, 2008, **361**, 4055; S. Bedoui, G. Molnar, S. Bonnet, H. J. Shepherd, W. Nicolazzi, L. Salmon and A. Bousseksou, *Chem. Phys. Lett.*, 2010, **499**, 94.

44 M. Lopes, C. M. Quintero, E. M. Hernandez, V. Velazquez, C. Bartual-Murgui, W. Nicolazzi, L. Salmon, G. Molnar and A. Bousseksou, *Nanoscale*, 2013, **5**, 7762.

45 S. Decurtins, P. Gütlich, C. P. Köhler, H. Spiering and A. Hauser, *Chem. Phys. Lett.*, 1984, **105**, 1; J. J. McGarvey and I. Lawthers, *J. Chem. Soc., Chem. Commun.*, 1982, 906; A. Hauser, *Chem. Phys. Lett.*, 1986, **124**, 543.

46 J. Kusz, H. Spiering and P. Gütlich, *J. Appl. Crystallogr.*, 2000, **33**, 201; J. Kusz, H. Spiering and P. Gütlich, *J. Appl. Crystallogr.*, 2001, **34**, 229.

47 M. Marchivie, P. Guionneau, J. A. K. Howard, G. Chastanet, J. F. Létard, A. E. Goeta and D. Chasseau, *J. Am. Chem. Soc.*, 2002, **124**, 194.

48 G. S. Matouzenko, S. A. Borshch, V. Schunemann and J. A. Wolny, *Phys. Chem. Chem. Phys.*, 2013, **15**, 7411.

49 V. Legrand, S. Pillet, H. P. Weber, M. Souhassou, J. F. Létard, P. Guionneau and C. Lecomte, *J. Appl. Crystallogr.*, 2007, **40**, 1076.

50 P. Guionneau and E. Collet, Piezo- and Photo-Crystallography Applied to Spin-Crossover Materials, in *Spin-Crossover Materials: Properties and Applications*, ed. M. A. Halcrow, John Wiley & Sons Ltd, Oxford, UK, 2013, ch. 20, 508.

51 E. Collet, M. Lorenc, M. Cammarata, L. Guérin, M. Servol, A. Tissot, M. L. Boillot, H. Cailleau and M. Buron-Le Cointe, *Chem.–Eur. J.*, 2012, **18**, 2051.

52 O. Kahn and C. Jay Martinez, *Science*, 1998, **279**, 44; P. Gütlich, Y. Garcia and T. Woike, *Coord. Chem. Rev.*, 2001, **219**, 839; J. F. Létard, P. Guionneau and L. Goux-Capes, *Top. Curr. Chem.*, 2004, **235**, 221.

53 C. P. Slichter and H. G. Drickamer, *J. Chem. Phys.*, 1972, **56**, 2142; V. Ksenofontov, A. B. Gaspar and P. Gütlich, *Top. Curr. Chem.*, 2004, **235**, 23; A. Bousseksou, G. Molnár, L. Salmon and W. Nicolazzi, *Chem. Soc. Rev.*, 2011, **40**, 3313; L. Stoleriu, P. Chakraborty, A. Hauser, A. Stancu and C. Enachescu, *Phys. Rev. B: Condens. Matter*, 2011, **84**, 134102; S. F. Matar and J. F. Létard, *Z. Naturforsch., B: Chem. Sci.*, 2010, **65**, 565.

54 A. Katrusiak, *Acta Crystallogr., Sect. A: Fundam. Crystallogr.*, 2008, **64**, 135; W. A. Basset, *High Pressure Res.*, 2009, **29**, 163; E. V. Boldyreva, *Acta Crystallogr., Sect. A: Fundam. Crystallogr.*, 2008, **64**, 218.

55 T. Granier, B. Gallois, J. Gaultier, J. A. Real and J. Zarembowitch, *Inorg. Chem.*, 1993, **32**, 5305.

56 V. Ksenofontov, G. Levchenko, H. Spiering, P. Gütlich, J.-F. Létard, Y. Bouhedja and O. Kahn, *Chem. Phys. Lett.*, 1998, **294**, 545–553; A. Rotaru, F. Varret, E. Codjovi, K. Boukheddaden, J. Linares, A. Stancu, P. Guionneau and J. F. Létard, *J. Appl. Phys.*, 2009, **106**, 053515.

57 V. Legrand, F. Le Gac, P. Guionneau and J. F. Létard, *J. Appl. Crystallogr.*, 2008, **47**, 637.

58 V. Legrand, S. Pechev, J. F. Létard and P. Guionneau, *Phys. Chem. Chem. Phys.*, 2013, **15**, 13872.

59 A. Marbeuf, S. F. Matar, P. Négrier, L. Kabalan, J. F. Létard and P. Guionneau, *Chem. Phys.*, 2013, **420**, 25.

60 H. J. Shepherd, P. Rosa, L. Vendier, N. Casati, J. F. Létard, A. Bousseksou, P. Guionneau and G. Molnar, *Phys. Chem. Chem. Phys.*, 2012, **14**, 5265.

61 H. J. Shepherd, T. Palamarciuc, P. Rosa, P. Guionneau, G. Molnar, J. F. Létard and A. Bousseksou, *Angew. Chem., Int. Ed.*, 2012, **51**, 3910.

62 A. Tissot, H. J. Shepherd, L. Toupet, E. Collet, J. Sainton, G. Molnár, P. Guionneau and M. L. Boillot, *Eur. J. Inorg. Chem.*, 2013, 1001.

63 G. Aromi, L. A. Barros, O. Roubeau and P. Gamez, *Coord. Chem. Rev.*, 2011, **255**, 485.

64 O. Roubeau, *Chem.–Eur. J.*, 2012, **18**, 15230.

65 C. Janiak, *Dalton Trans.*, 2003, 2781.

66 J. Kröber, J. P. Audière, R. Claude, E. Codjovi, O. Kahn, J. G. Haasnoot, F. Grolière, C. Jay, A. Bousseksou, J. Linarès, F. Varret and A. Gonthier-Vassal, *Chem. Mater.*, 1994, **6**, 1404.

67 L. G. Lavrenova and O. G. Shakirova, *Eur. J. Inorg. Chem.*, 2013, 670.

68 A. Michalowicz, J. Moscovici, B. Ducourant, D. Cracco and O. Kahn, *Chem. Mater.*, 1995, **6**, 1404; M. Verelst, L. Sommier, P. Lecante, A. Mosset and O. Kahn, *Chem. Mater.*, 1998, **10**, 980.

69 A. Urakawa, W. V. Beek, M. Monrabal-Capilla, J. R. Galan-Mascaros, L. Palin and M. Milanesio, *J. Phys. Chem. C*, 2011, **115**, 1323; M. M. Dirtu, C. Neuhausen, A. D. Naik, A. Rotaru, L. Spinu and Y. Garcia, *Inorg. Chem.*, 2010, **49**, 5723.

70 A. Grosjean, N. Daro, B. Kauffmann, A. Kaiba, J. F. Létard and P. Guionneau, *Chem. Commun.*, 2011, **47**, 12382.

71 P. Durand, S. Pillet, E. Bendeif, C. Carteret, M. Bouazaoui, H. El Hamzaoui, B. Capoen, L. Salmon, S. Hébert, J. Ghanbaja, L. Aranda and D. Schaniel, *J. Mater. Chem.*, 2013, **1**, 1933; E. Coronado, J. R. Galán-Mascarós, M. Monrabal-Capilla, J. García-Martínez and P. Pardo-Ibáñez, *Adv. Mater.*, 2007, **19**, 1359.

72 T. Forestier, A. Kaiba, S. Pechev, D. Denux, P. Guionneau, C. Etrillard, N. Daro, E. Freysz and J. F. Létard, *Chem.–Eur. J.*, 2009, **15**, 6122.

73 K. S. Murray, H. Oshio and J. A. Real, *Eur. J. Inorg. Chem.*, 2013, 577.

74 A. Gavezzotti, *Acc. Chem. Res.*, 1994, **27**, 309.